

Published in final edited form as:

Nat Genet. 2006 July ; 38(7): 801–806. doi:10.1038/ng1814.

Mutations in the human GlyT2 gene define a presynaptic component of human startle disease

Mark I. Rees^{1,3,†}, Kirsten Harvey^{2,†}, Brian R. Pearce², Seo-Kyung Chung^{1,3}, Ian C. Duguid⁴, Philip Thomas⁴, Sarah Beatty³, Gail E. Graham⁵, Linlea Armstrong⁶, Rita Shiang⁷, Kim J. Abbott⁸, Sameer M. Zuberi⁹, John B.P. Stephenson⁹, Michael J. Owen¹⁰, Marina A.J. Tijssen¹¹, Arn M.J.M. van den Maagdenberg¹², Trevor G. Smart⁴, Stéphane Supplisson¹³, and Robert J. Harvey²

¹School of Medicine, University of Wales Swansea, Singleton Park, West Glamorgan SA2 8PP, UK ²Dept. of Pharmacology, The School of Pharmacy, 29-39 Brunswick Square, London WC1N 1AX, UK ³Dept. of Molecular Medicine, Faculty of Medical and Health Sciences, University of Auckland, Private bag 92019, Auckland, New Zealand ⁴Dept. of Pharmacology, University College London, Gower Street, London WC1E 6BT, UK ⁵Dept. of Genetics, Children's Hospital of Eastern Ontario, 401 Smyth Rd, Ontario K1H 8L1, Canada ⁶Dept. of Medical Genetics, Children's and Women's Health Centre of British Columbia, 4500 Oak Street, Vancouver, British Columbia V6H 3N1, Canada ⁷Dept. of Human Genetics, Virginia Commonwealth University Medical Center, P.O. Box 980033, Richmond, VA 23298-0033, USA ⁸Women's and Children's Hospital, 72 King William Road, Adelaide, Australia ⁹Fraser of Allander Neurosciences Unit, Royal Hospital for Sick Children, Glasgow, G3 8SJ, UK ¹⁰Psychological Medicine, University of Wales College of Medicine, Cardiff CF14 4XN, UK ¹¹Dept. of Neurology, Academic Medical Centre, University of Amsterdam, PO BOX 22660, 1100 DD Amsterdam, The Netherlands ¹²Dept. of Neurology and Dept. of Human Genetics, Leiden University Medical Centre, PO Box 9600, 2300 RC Leiden, The Netherlands ¹³Laboratoire de Neurobiologie, CNRS UMR8544, Ecole Normale Supérieure, 46 Rue d'Ulm, 75005 Paris, France

Abstract

Hyperekplexia is a human neurological disorder characterized by an excessive startle response and is typically caused by missense and nonsense mutations in the gene encoding the inhibitory glycine receptor (GlyR) $\alpha 1$ subunit (*GLRA1*)¹⁻³. Genetic heterogeneity has been confirmed in isolated sporadic cases with mutations in other postsynaptic glycinergic proteins including the GlyR β subunit (*GLRB*)⁴, gephyrin (*GPHN*)⁵ and RhoGEF collybistin (*ARHGEF9*)⁶. However, many sporadic patients diagnosed with hyperekplexia do not carry mutations in these genes²⁻⁷. Here we reveal that missense, nonsense and frameshift mutations in the presynaptic glycine transporter 2 (GlyT2) gene (*SLC6A5*)⁸ also cause hyperekplexia. Patients harbouring mutations in *SLC6A5* presented with hypertonia, an exaggerated startle response to tactile or acoustic stimuli, and life-threatening neonatal apnoea episodes. GlyT2 mutations result in defective subcellular localisation and/or decreased glycine uptake, with selected mutations affecting predicted glycine and Na⁺ binding sites. Our results demonstrate that *SLC6A5* is a major gene for hyperekplexia and define the first neurological disorder linked to mutations in a Na⁺/Cl⁻-dependent transporter for a classical fast neurotransmitter. By analogy, we suggest that in other human disorders where

Correspondence and requests for materials (subject to a Material Transfer Agreement) should be addressed to R.J.H. (robert.harvey@pharmacy.ac.uk) or M.I.R. (m.i.rees@swansea.ac.uk).

[†]these authors contributed equally to this work.

COMPETING INTERESTS STATEMENT: The authors declare that they have no competing financial interests.

defects in postsynaptic receptors have been identified, similar symptoms could result from defects in the cognate presynaptic neurotransmitter transporter.

Glycine transporters (GlyTs) are members of the Na⁺/Cl⁻-dependent neurotransmitter transporter superfamily^{9,10}, integral membrane proteins that utilise electrochemical gradients to control the concentration of neurotransmitters at central synapses. This superfamily also includes transporters for GABA, biogenic amines (norepinephrine, dopamine, serotonin, proline), betaine, taurine and creatine. GlyTs have dual functions at both inhibitory and excitatory synapses, resulting from the differential localisation of two distinct transporters^{9,10}, GlyT1 and GlyT2. GlyT1 is predominantly expressed in glial cells^{9,10}, exhibits a 2 Na⁺/1 Cl⁻/1 glycine stoichiometry and bi-directional glycine transport¹¹. These properties are appropriate for the control of extracellular glycine concentrations in the submicromolar range for modulation of *N*-methyl-D-aspartate receptors¹², and also for lowering extracellular glycine levels at inhibitory glycinergic synapses^{13,14}. By contrast, GlyT2 is found in glycinergic axons, exhibits a 3 Na⁺/1 Cl⁻/1 glycine stoichiometry and does not display reverse uptake¹¹, reflecting an essential role for GlyT2 in maintaining a high presynaptic pool of neurotransmitter at glycinergic synapses¹⁵. Na⁺/Cl⁻-dependent transporters are known drug targets (e.g. for anticonvulsants¹⁶ or selective serotonin reuptake inhibitors¹⁷, SSRIs) and drugs of abuse (e.g. cocaine, amphetamine). For this reason, genetic variation in human transporter genes has been studied in a variety of disorders including Parkinson's disease¹⁸, depression¹⁸, orthostatic intolerance¹⁹ and epilepsy²⁰. Although mutations in the human creatine transporter gene (*SLC6A8*) on chromosome Xq28 are associated with mental retardation^{21,22}, no genetic defects in classical Na⁺/Cl⁻-dependent neurotransmitter transporters (i.e. GABA, serotonin, glycine) have been directly related to pathogenic human disorders. Nevertheless, we considered that neurological disorders with a postsynaptic genetic component might also have a corresponding undiscovered presynaptic defect. For example, hereditary hyperekplexia (*STHE*: OMIM 149400) is a rare, but potentially lethal condition, typically caused by mutations in the gene for the glycine receptor (GlyR) α 1 subunit (*GLRA1*)¹⁻³. Despite isolated hyperekplexia cases harbouring mutations in the GlyR β subunit (*GLRB*)⁴, and the clustering proteins gephyrin (*GPHN*)⁵ and collybistin (*ARHGGEF9*)⁶, for many sporadic patients no causative mutation has been identified²⁻⁷. Since knockout mice for the presynaptic Na⁺/Cl⁻-dependent transporter GlyT2 have been reported¹⁵ to display a phenotype similar to hyperekplexia, as part of an ongoing screening programme we assessed whether defects in the human GlyT2 gene (*SLC6A5*) could cause this disorder.

We scanned all 16 coding exons of the *SLC6A5* gene (11p15.1) by dHPLC analysis (for primers see Supplementary Table 1 online) in an international cohort of 83 sporadic and familial hyperekplexia patients²⁻⁷ devoid of mutations in *GLRA1*, *GLRB*, *GPHN* and *ARHGGEF9* (Supplementary Table 2 online). Direct sequencing of aberrant dHPLC profiles revealed a mosaic of missense and nonsense mutations in *SLC6A5* (Table 1, Fig. 1 and Supplementary Fig. 1 online) and additional regions of high-frequency SNPs (Supplementary Table 3 online). All mutations in Table 1 have been excluded from 400 unrelated, normal control chromosomes. In the majority of cases (5/6), GlyT2 mutations were inherited as compound heterozygotes indicating that *SLC6A5* is predominantly associated with recessive hyperekplexia (Table 1 and Fig. 1). A nonsense mutation (Y377X) plus a mixed missense/frameshift mutation (V432F+fs97) were detected in patient 1, a severely affected individual with compound inheritance of null alleles. In the mother, the V432F+fs97 mutation segregates with a partial form of hyperekplexia, associated with nocturnal myoclonus and a nervous disposition. However, the paternal allele Y377X does not evoke a hyperekplexia phenotype. Compound heterozygosity in patient 2 is represented by nonsense (Q630X) and missense (Y491C) mutations. The origin of these alleles could

not be determined in the unaffected parents since they declined to participate in this study. However, long-distance PCR from exons 9 and 13 and subsequent cloning of PCR products revealed that these alleles reside on different chromosomes. Two sibling brothers with hyperekplexia are represented by patient 3, and both inherited a missense/frameshift (P108L+fs25) and missense (W482R) mutations from their unaffected parents. Patient 4 inherited two missense mutations L306V and N509S, whilst patient 5 is homozygous for a single missense mutation (T425M) inherited from consanguineous parents. Finally, a maternal missense mutation (S510R) was also identified in patient 6. Although a paternal sequence variation (A89E) was identified, we could exclude the possibility of compound heterozygosity because this variant was also detected in 4/203 control samples. All patients harbouring mutations in *SLC6A5* presented with classical hyperekplexia symptoms (see Supplementary note and Video for patient 6 online) including neonatal muscle hypertonia and an exaggerated startle response to tactile or acoustic stimuli with preservation of consciousness. However, in contrast to most patients harbouring mutations in *GLRA1*, individuals with *SLC6A5* mutations showed prolonged spasms with life-threatening neonatal apnoea and breath-holding episodes. Notably, in some cases, symptoms resolved within the first year of life.

To confirm the pathogenicity of these alleles, we performed a series of functional tests using recombinant expression of human GlyT2 and mutants produced by site-directed mutagenesis. These experiments included assessment of cell-surface localisation and capacity for [³H]glycine uptake in HEK293 cells, together with electrophysiological measurements of glycine-evoked steady-state currents in *Xenopus* oocytes. Non-mutated EGFP- or myc-tagged hGlyT2 as well as A89E, L306V, T425M, W482R, Y491C and N509S were readily expressed at the cell surface (Fig. 2a). By contrast, frameshift (P108L+fs25 and V432F+fs97) and nonsense (Y377X and Q630X) mutations were clearly cytoplasmic, suggesting that protein truncation results in a loss of cell surface GlyT2. S510R was also cytoplasmic, but formed intracellular aggregates (Fig. 2a,b) which readily trap co-transfected myc-tagged hGlyT2 (Fig. 2b), supporting a dominant-negative mode of action. Consistent with these findings, mutations P108L+fs25, Y377X, V432F+fs97, Q630X and S510R abolished [³H]glycine uptake (Fig. 3a). Despite reaching the cell surface, transporters harbouring mutations T425M, W482R, Y491C and N509S also revealed no significant [³H]glycine uptake, while A89E and L306V resembled EGFP-hGlyT2 (Fig. 3a). Taken together, these data provide strong evidence for a bi-allelic loss of GlyT2 function in patients 1 (Y377X plus V432F+fs97), 2 (Q630X plus Y491C), 3 (P108L+fs25 plus W482R) and 5 (homozygous for T425M). However, the mechanisms underlying the clinical phenotype in patients 4 (L306V plus N509S) and 6 (heterozygous for S510R) remained ambiguous. We therefore tested whether co-transfection of the two alleles would provide evidence for dominant or synergistic effects, since intracellular heteromeric GlyT2 assembly has been reported, although cell-surface GlyT2 is presumed to be monomeric²³. Mixing N509S or L306V with EGFP-hGlyT2 did not substantially alter [³H]glycine uptake, but co-transfection of N509S and L306V completely negated uptake (Fig. 3b). This suggests that *in vivo* N509S/L306V mutant polypeptides act synergistically to cause bi-allelic GlyT2 dysfunction, compatible with a recessive mode of inheritance. Consistent with cytoplasmic trapping of myc-tagged GlyT2 by EGFP-hGlyT2S510R (Fig. 2b), co-expression of S510R with hGlyT2 or A89E resulted in the loss of [³H]glycine uptake (Fig. 3b), providing further evidence that S510R is a dominant-negative mutation.

Insights into the precise molecular mechanisms underlying GlyT2 missense mutations were provided by homology modelling of GlyT2 using the crystal structure of the bacterial leucine transporter (LeuT)²⁴. Alignment of the *Aquifex aeolicus* LeuT with GlyT1 and GlyT2 allowed residues potentially involved in co-ordinating glycine and Na⁺ binding to be identified. In particular, we predicted that mutations W482R (TM6) and N509S (TM7)

could disrupt glycine or Na⁺ binding to GlyT2, respectively (Fig. 1a-c). Two-electrode voltage clamp analysis in *Xenopus* oocytes demonstrated the mutant W482R does not respond to glycine (up to 10 mM). However, the mutant W482R was clearly present at the cell surface, as demonstrated by Na⁺-dependent transient currents^{9,25} which were glycine insensitive, but blocked by ORG25543 (a specific GlyT2 inhibitor; Fig. 4a-c, e). By contrast, neither transient nor glycine-induced currents could be detected for mutants T425M, Y491C or S510R. This confirms our prior [³H]glycine uptake results (Fig. 3a) and suggested that while T425M and Y491C reach the cell surface (Fig. 2a), they are not functional. Transient and steady state-currents, which are related to transporter expression^{26,27} were observed for L306V and for N509S. However, disruption of the highly conserved residue N509 produced a dramatic and voltage-dependent decrease in glycine potency (Fig. 4b-c) from $26.9 \pm 3.3 \mu\text{M}$ (hGlyT2) to $1923.8 \pm 227.7 \mu\text{M}$ (N509S) at -40mV (Fig. 3c). Similar results were obtained for glycine-activated currents for hGlyT2 and N509S expressed in NG108 cells (Supplementary Fig. 2 online, EC₅₀ for hGlyT2, $27.4 \pm 2.4 \mu\text{M}$; N509S, $2651 \pm 417 \mu\text{M}$ at -50mV). These shifts in potency are sufficient to account for the apparent lack of glycine uptake for N509S in HEK293 cells (Fig. 3a; assayed using $200 \mu\text{M}$ glycine) and demonstrated that while N509S may impair Na⁺-glycine coupling, mutation L306V alone did not substantially impair transporter function. Current/voltage relationships for N509S and L306V in oocytes are similar to hGlyT2, showing that these mutants conserved a high thermodynamic coupling between glycine-evoked current and glycine uptake (Fig. 4d). The charge movement (Q_v) across the oocyte membrane associated with the activation of GlyT2 was assessed by measuring the integrals of the transient currents at different voltage-clamp holding potentials (V_m). The resulting Q_v - V_m relationships were fitted with the Boltzmann equation and revealed that all possessed similar equivalent charges ($z\delta$) to hGlyT2, suggesting no change in the number of Na⁺ ions that are bound to the transporter. However, the holding potential at which the charge transfer is half the maximum ($V_{0.5}$) for all three GlyT2 mutants was shifted to hyperpolarized potentials, in accord with a reduced apparent affinity for Na⁺ (Fig. 4e).

In conclusion, it is apparent that hyperekplexia is principally caused by defects in glycinergic transmission, which conspire to alter either postsynaptic receptor function and/or location, or presynaptic mechanisms involved in vesicular replenishment. Although mouse knockouts for GlyT2 have been suggested¹⁵ to exhibit a behavioural phenotype similar to human hyperekplexia, there are several marked differences to patients harbouring mutations in *SLC6A5*. GlyT2 knockout mice gain weight slowly and die prematurely at the end of the second postnatal week, displaying a complex neurological phenotype characterised by spasticity, rigid muscle tone, strong tremor and a severely impaired righting reflex. Importantly, GlyT2 knockout mice develop strong spontaneous tremor and increased muscle tone. By contrast, patients harbouring GlyT2 mutations show no spontaneous tremor or muscle stiffness, but this can be triggered by acoustic or tactile stimuli. In the hierarchical genetic analysis of hyperekplexia, *SLC6A5* must now be regarded as a major candidate gene and have equal priority to *GLRA1* screening. GlyT2 accessory proteins (such as the PDZ domain containing protein syntenin-1 and ULIP6) that are involved in the correct localisation of GlyT2 at presynaptic terminals^{28,29}, must also be considered as candidates for the remaining hyperekplexia patients awaiting a definitive genetic diagnosis. Lastly, while mutations in *SLC6A5* should be regarded as a sudden infant death syndrome risk-factor (due to developmentally-specific anoxic seizures and cyanotic syncope), symptoms often resolve during a period of developmental transience from early postnatal months into infancy.

METHODS

Mutation screening of the human GlyT2 gene (SLC6A5)

In total, 83 samples were screened for *SLC6A5* mutations, all of which have proved gene-negative in screens³⁻⁶ of *GLRA1*, *GLRB*, *GPHN* and *ARHGEF9*. Four samples represented two sets of asymptomatic parents from an affected child, whilst three samples were members of a large family with one severely affected index case. The remaining 76 samples were all single unrelated sporadic cases from neurological or genetics clinic referrals. Ethical approval for the genetic testing of patients with epilepsy and paroxysmal disorders is held with the Auckland Regional Ethical Committee in New Zealand (MIR). Written patient/parental consent for blood samples and subsequent gene screening is held with the referring clinicians in accordance with individual national ethical requirements. Patient and physician written consent was a study prerequisite, but due to the global and multi-national origin of DNA samples, the consent format was not standardised. *SLC6A5* exons, flanking intronic sequences, plus 5' and 3' untranslated regions were derived *in silico*, using the Human Genome Browser at UCSC (<http://genome.ucsc.edu/>). PCRs were performed on patient genomic DNAs using primers described in Supplementary table 1. Each 25 μ l reaction contained 60 ng of genomic DNA, 10 pmol of each primer, 1.5 mM MgCl₂, 50 mM KCl, 10 mM Tris-HCl pH 8.3, 200 μ M of dNTPs and 1 U *Taq* polymerase (Qiagen). PCR conditions were 94°C for 5 min followed by 35 cycles of 30 s at 94°C, 30 s at 60°C, 30 s at 72°C. Mutation screening of PCR products were performed using a Transgenomics dHPLC HT-WAVE^R DNA Fragment Analysis System, using DNASep^R columns (Transgenomics), under partially denaturing conditions for mutation detection and SNP discovery. Aberrant dHPLC profiles were gel-isolated (QIAGEN) and sequenced using ABI3100 and BigDye ready reaction technology (Applied Biosystems). Population studies were conducted using RFLP analysis or, in the absence of a restriction site assay, dHPLC profiles of controls were analyzed with a mutation-positive control.

Amplification, cloning and mutagenesis of human GlyT2 cDNAs

Human GlyT2 cDNAs were amplified from human hippocampal cDNA (Clontech) using the primers hGlyT2A-1 and hGlyT2A-2 (Supplementary table 1) and 30 cycles of 94°C for 1 min, 60°C for 1 min and 68°C for 6 min. PCR products were cloned into the *Eco*RI and *Xho*I sites of the vector pcDNA3 (Invitrogen) and twelve full-length cDNAs were sequenced. hGlyT2-1 has an SNP background of G102, S104, K457 and D463 (Supplementary table 2). The insert from one of these clones, pcDNA3-hGlyT2-1 was subcloned into three additional vectors: pEGFP-C1 (Clontech; resulting in construct pEGFP-hGlyT2, N-terminal EGFP tag), pRK5myc (resulting in construct pRK5myc-GlyT2, N-terminal myc tag) and pRC/CMV (Invitrogen; resulting in plasmid pRC/CMV-hGlyT2). GlyT2 mutations were introduced into these plasmids using the Quikchange site directed mutagenesis kit (Stratagene). The coding region of each construct was fully sequenced using the BigDye ready reaction mix (Perkin-Elmer/Applied Biosystems) and an Applied Biosystems 310 automated DNA sequencer to verify that only the desired mutation had been introduced.

Glycine uptake assays

HEK293 cells (ATCC CRL1573) were plated onto poly-D-lysine-coated 24-well plates (Nunc) and grown to 50% confluence in MEM (Earles salts) supplemented with 10% (v/v) FCS, 2 mM L-glutamine and 20 U/ml penicillin/streptomycin in 5% CO₂/air. Cells were transfected with 0.25 μ g total pEGFP-C1 (control), pEGFP-hGlyT2 or mutant DNA per well using Effectene (Qiagen). After 24h, cells were washed with a buffer containing 116 mM NaCl, 1 mM NaH₂PO₄, 26 mM NaHCO₃, 1.5 mM MgSO₄, 5 mM KCl, 1.3 mM CaCl₂ and 5 mM glucose pre-gassed with 5% CO₂/air, then incubated for 5 min in 1 μ Ci/ml ³H-glycine

(60 Ci/mmol, NEN) at a final concentration of 200 μ M. Uptake was terminated by two additions of ice-cold buffer followed by aspiration. Cells were digested in 0.1 M NaOH and used for scintillation counting and determination of protein concentration using Bradford reagent (BioRad). 3 H-glycine uptake was calculated as nmoles/min/mg protein and expressed as a percentage of the pEGFP-C1 transfected control. Glycine uptake into control cultures was found to be 0.46 nmoles/min/mg protein ($n = 20$). The kinetics of 3 H-glycine uptake were determined with pEGFP-hGlyT2 expressing cells in the presence of 1-1000 μ M unlabelled glycine. This revealed a K_m of 66 μ M and V_{max} of 1.64 nmoles/min/mg protein. All statistical comparisons used an unpaired Students t-test.

GlyT2 subcellular localization

HEK293 cells were electroporated (400V, infinite resistance, 125 μ F; BioRad Gene Electropulser II) with pEGFP-hGlyT2 (wild-type) or mutant plasmids. After 24 h, cells were washed twice in PBS, fixed for 5 min in 4% (w/v) PFA in PBS and quenched in 50 mM NH_4Cl for 10 min before further washing in PBS. Confocal microscopy was performed using a Zeiss Axioscop LSM 510 Meta confocal microscope with 40 \times objective (N.A. 1.3) and 3 \times digital zoom. Images (1024 \times 1024 pixel resolution) were acquired following laser excitation (488 nm) of a 0.9 μ m optical section and stored offline for further analysis. Each mutant was transfected at least four times, and images were obtained from at least four cells per mutant. Phenotypes shown were present in >85% of transfected cells. Cells showing extreme levels of exogenous protein expression, significant cell volume loss or other signs of cell death were discounted from image analysis.

Electrophysiological analysis of GlyT2 mutants

Xenopus oocytes were prepared as previously described⁹. cRNAs coding for wild-type GlyT2 and each mutant were synthesized *in vitro* from pRC/CMV-hGlyT2 constructs (mMessage-mMachine, AMBION) and ~50 ng of mRNA was injected into *Xenopus* oocytes. Three to seven days after mRNA injection, oocytes were held at -40 mV with a two-microelectrode voltage-clamp amplifier (WARNER OC725C) and continuously perfused with Ringer solution (100mM NaCl, 1.8mM $CaCl_2$, 1mM $MgCl_2$, 5mM HEPES, pH 7.4 with KOH). Currents were filtered at 1 kHz before digitalization at 5kHz (Digidata 1200, Axon Instruments, PClamp 8). NG108-15 cells were grown under non-differentiating conditions in MEM (Earles salts) with 10% (v/v) FCS, 4 mM L-glutamine, 1.13% (v/v) glucose, 20 U/ml penicillin/streptomycin and 2% HAT media supplement (50 \times) in 5% CO_2 /air. Cells were plated onto poly-ornithine coated coverslips and transfected using calcium phosphate with cDNAs for GlyT2 and EGFP. Whole-cell glycine-evoked currents, normalised to cell capacitance, were recorded up to 16h later (20-22 $^{\circ}C$) from single NG108 cells voltage-clamped at -50 mV, with an Axopatch 200B (Axon Instruments) and filtered (8-pole Bessel) at 2 kHz prior to digitisation (Digidata 1320A). Patch electrodes (3-5 M Ω) contained (mM): 140 K^+ -gluconate, 1 $MgCl_2$, 1 $CaCl_2$, 10 HEPES, 11 EGTA and 5 adenosine triphosphate, pH 7.2. Cells were continuously superfused with Krebs solution containing: 140mM NaCl, 4.7mM KCl, 1.2mM $MgCl_2$, 2.5mM $CaCl_2$, 10mM HEPES and 11mM glucose, pH 7.4. All solutions were applied using a modified U-tube. Data were analysed using Clampfit 8.2 (Axon) and Origin 6 (Microcal). Dose-response relationships were fitted with the Hill equation. All data points represent the mean \pm s.e.

Supplementary Material

Refer to Web version on PubMed Central for supplementary material.

Acknowledgments

We thank Dr E.A. Peeters (Juliana Pediatric Hospital, The Hague, The Netherlands) and Dr K. Braun (Pediatric Neurology, Utrecht Medical Centre, The Netherlands) for patient referrals. This work was supported by grants from the Medical Research Council (United Kingdom) to RJH and TGS, the Neurological Foundation for New Zealand and Auckland Medical Research Foundation to MIR and from Fédération pour la Recherche sur le Cerveau and Association Française contre les Myopathies to SS.

REFERENCES

- Shiang R, Ryan SG, Zhu YZ, Hahn AF, O'Connell P, Wasmuth JJ. Mutations in the $\alpha 1$ subunit of the inhibitory glycine receptor cause the dominant neurologic disorder, hyperekplexia. *Nat. Genet.* 1993; 5:351–358. [PubMed: 8298642]
- Shiang R, Ryan SG, Zhu YZ, Fielder TJ, Allen RJ, Fryer A, Yamashita S, O'Connell P, Wasmuth JJ. Mutational analysis of familial and sporadic hyperekplexia. *Ann. Neurol.* 1995; 38:85–91. [PubMed: 7611730]
- Rees MI, Lewis TM, Vafa B, Ferrie C, Corry P, Muntoni F, Jungbluth H, Stephenson JB, Kerr M, Snell RG, Schofield PR, Owen MJ. Compound heterozygosity and nonsense mutations in the $\alpha 1$ -subunit of the inhibitory glycine receptor in hyperekplexia. *Hum. Genet.* 2001; 109:267–270. [PubMed: 11702206]
- Rees MI, Lewis TM, Kwok JB, Mortier GR, Govaert P, Snell RG, Schofield PR, Owen MJ. Hyperekplexia associated with compound heterozygote mutations in the β -subunit of the human inhibitory glycine receptor (*GLRB*). *Hum. Mol. Genet.* 2002; 11:853–860. [PubMed: 11929858]
- Rees MI, Harvey K, Ward H, White JH, Evans L, Duguid IC, Hsu CC, Coleman SL, Miller J, Baer K, Waldvogel HJ, Gibbon F, Smart TG, Owen MJ, Harvey RJ, Snell RG. Isoform heterogeneity of the human gephyrin gene (*GPHN*), binding domains to the glycine receptor, and mutation analysis in hyperekplexia. *J. Biol. Chem.* 2003; 278:24688–24696. [PubMed: 12684523]
- Harvey K, Duguid IC, Alldred MJ, Beatty SE, Ward H, Keep NH, Lingenfelter SE, Pearce BR, Lundgren J, Owen MJ, Smart TG, Luscher B, Rees MI, Harvey RJ. The GDP-GTP exchange factor collybistin: an essential determinant of neuronal gephyrin clustering. *J. Neurosci.* 2004; 24:5816–5826. [PubMed: 15215304]
- Vergouwe MN, Tijssen MA, Shiang R, van Dijk JG, al Shahwan S, Ophoff RA, Frants RR. Hyperekplexia-like syndromes without mutations in the *GLRA1* gene. *Clin. Neurol. Neurosurg.* 1997; 99:172–178. [PubMed: 9350397]
- Morrow JA, Collie IT, Dunbar DR, Walker GB, Shahid M, Hill DR. Molecular cloning and functional expression of the human glycine transporter GlyT2 and chromosomal localisation of the gene in the human genome. *FEBS Lett.* 1998; 439:334–340. [PubMed: 9845349]
- Roux MJ, Supplisson S. Neuronal and glial glycine transporters have different stoichiometries. *Neuron.* 2000; 25:373–383. [PubMed: 10719892]
- Eulenburg V, Arnsen W, Betz H, Gomeza J. Glycine transporters: essential regulators of neurotransmission. *Trends Biochem. Sci.* 2005; 30:325–333. [PubMed: 15950877]
- Supplisson S, Roux MJ. Why glycine transporters have different stoichiometries. *FEBS Lett.* 2002; 529:93–101. [PubMed: 12354619]
- Gabernet L, Pauly-Evers M, Schwerdel C, Lentz M, Bluethmann H, Vogt K, Alberati D, Möhler H, Boison D. Enhancement of the NMDA receptor function by reduction of glycine transporter 1 expression. *Neurosci. Lett.* 2005; 373:79–84. [PubMed: 15555781]
- Gomeza J, Hulsmann S, Ohno K, Eulenburg V, Szoke K, Richter D, Betz H. Inactivation of the glycine transporter 1 gene discloses vital role of glial glycine uptake in glycinergic inhibition. *Neuron.* 2003; 40:785–796. [PubMed: 14622582]
- Tsai G, Ralph-Williams RJ, Martina M, Bergeron R, Berger-Sweeney J, Dunham KS, Jiang Z, Caine SB, Coyle JT. Gene knockout of glycine transporter 1: characterization of the behavioural phenotype. *Proc. Natl. Acad. Sci. USA.* 2004; 101:8485–8490. [PubMed: 15159536]
- Gomeza J, Ohno K, Hulsmann S, Arnsen W, Eulenburg V, Richter DW, Laube B, Betz H. Deletion of the mouse glycine transporter 2 results in a hyperekplexia phenotype and postnatal lethality. *Neuron.* 2003; 40:797–806. [PubMed: 14622583]

16. Krogsgaard-Larsen P, Frolund B, Frydenvang K. GABA uptake inhibitors. Design, molecular pharmacology and therapeutic aspects. *Curr. Pharm. Des.* 2000; 6:1193–1209. [PubMed: 10903390]
17. Barker, EL.; Blakely, RD. *Psychopharmacology - the Fourth Generation of Progress*. Bloom, FE.; Kupfer, DJ., editors. Raven Press; New York: 2000.
18. Hahn MK, Blakely RD. Monoamine transporter gene structure and polymorphisms in relation to psychiatric and other complex disorders. *Pharmacogenomics J.* 2002; 2:217–235. [PubMed: 12196911]
19. Hahn MK, Mazei-Robison MS, Blakely RD. Single nucleotide polymorphisms in the human norepinephrine transporter gene affect expression, trafficking, antidepressant interaction, and protein kinase C regulation. *Mol. Pharmacol.* 2005; 68:457–466. [PubMed: 15894713]
20. Richerson GB, Wu Y. Role of the GABA transporter in epilepsy. *Adv. Exp. Med. Biol.* 2004; 548:76–91. [PubMed: 15250587]
21. Hahn KA, Salomons GS, Tackels-Horne D, Wood TC, Taylor HA, Schroer RJ, Lubs HA, Jacobs C, Olson RL, Holden KR, Stevenson RE, Schwartz CE. X-linked mental retardation with seizures and carrier manifestations is caused by mutation in the creatine-transporter gene (*SLC6A8*) located in Xq28. *Am. J. Hum. Genet.* 2002; 70:1349–1356. [PubMed: 11898126]
22. Rosenberg EH, Almeida LS, Kleefstra T, deGrauw RS, Yntema HG, Bahi N, Moraine C, Ropers HH, Fryns JP, deGrauw TJ, Jakobs C, Salomons GS. High prevalence of SLC6A8 deficiency in X-linked mental retardation. *Am. J. Hum. Genet.* 2004; 75:97–105. [PubMed: 15154114]
23. Horiuchi M, Nicke A, Gomeza J, Aschrafi A, Schmalzing G, Betz H. Surface-localized glycine transporters 1 and 2 function as monomeric proteins in *Xenopus* oocytes. *Proc. Natl. Acad. Sci. USA.* 2001; 98:1448–1453. [PubMed: 11171971]
24. Yamashita A, Singh SK, Kawate T, Jin Y, Gouaux E. Crystal structure of a bacterial homologue of Na⁺/Cl⁻-dependent neurotransmitter transporters. *Nature.* 2005; 437:215–223. [PubMed: 16041361]
25. Roux MJ, Martinez-Maza R, Le Goff A, Lopez-Corcuera B, Aragon C, Supplisson S. The glial and the neuronal glycine transporters differ in their reactivity to sulfhydryl reagents. *J. Biol. Chem.* 2001; 276:17699–17705. [PubMed: 11278474]
26. Mager S, Naeve J, Quick M, Labarca C, Davidson N, Lester HA. Steady states, charge movements, and rates for a cloned GABA transporter expressed in *Xenopus* oocytes. *Neuron.* 1993; 10:177–188. [PubMed: 7679914]
27. Mager S, Kleinberger-Doron N, Keshet GI, Davidson N, Kanner BI, Lester HA. Ion binding and permeation at the GABA transporter GAT1. *J. Neurosci.* 1996; 16:5405–5414. [PubMed: 8757253]
28. Ohno K, Koroll M, El Far O, Scholze P, Gomeza J, Betz H. The neuronal glycine transporter 2 interacts with the PDZ domain protein syntrophin-1. *Mol. Cell. Neurosci.* 2004; 26:518–529. [PubMed: 15276154]
29. Horiuchi M, Loeblich S, Brandstaetter JH, Kneussel M, Betz H. Cellular localization and subcellular distribution of Unc-33-like protein 6, a brain-specific protein of the collapsing response mediator protein family that interacts with the neuronal glycine transporter 2. *J. Neurochem.* 2005; 94:307–315. [PubMed: 15998282]
30. Tunncliffe G. Membrane glycine transport proteins. *J. Biomed. Sci.* 2003; 10:30–36. [PubMed: 12566983]

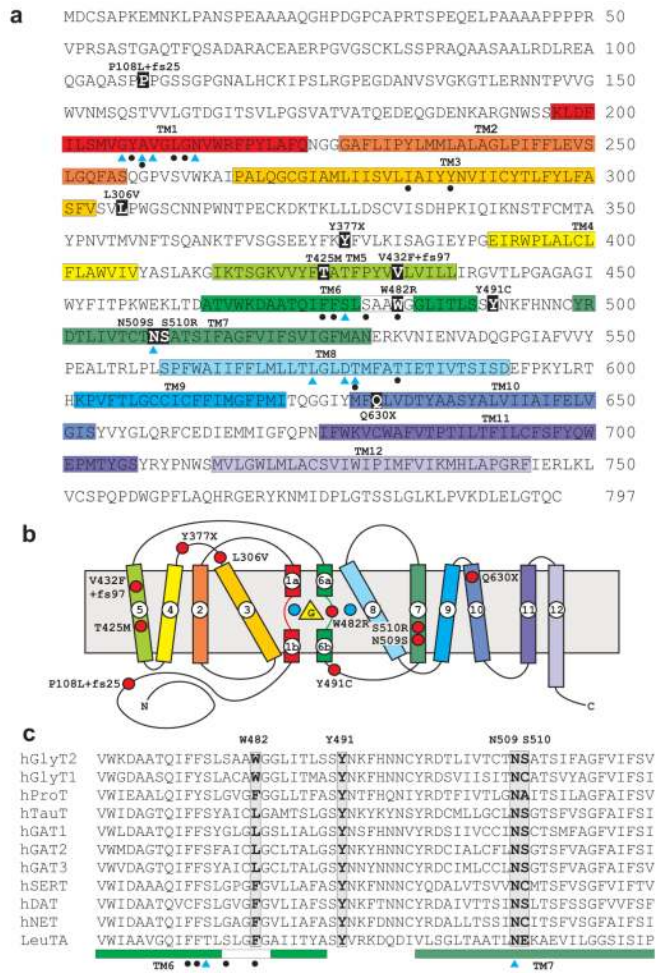


Fig. 1. Amino acid sequence of human GlyT2 indicating mutations identified in hyperkplexia
a, Amino acid sequence of human GlyT2 indicating the revised positions of putative transmembrane (TM) domains (coloured boxes). Blue triangles show residues in hGlyT2 that are likely to co-ordinate Na⁺ ions based on sequence alignments with the bacterial leucine transporter LeuT²⁴. This involves residues in TM1 (G206, A208, V209, N213), TM6 (S477), TM7 (N509) and TM8 (L574, D577, T578). However, it is noteworthy that GlyT2 binds three Na⁺ ions, while LeuT binds two, suggesting that other residues involved in Na⁺ co-ordination remain to be identified. Filled black circles indicate residues predicted to be involved in glycine binding, including residues in TM1 (Y207, A208, L211, G212), TM3 (I283, Y287), TM6 (F475, F476, S479, W482) and TM8 (T578, T582). **b**, Schematic diagram showing the suggested topology of GlyT2 and relative positions of GlyT2 mutations (red circles), adapted from Yamashita et al²⁴. The positions of glycine and two of the three sodium ions are depicted by a yellow triangle and blue circles, respectively. **c**, alignment of the TM6-TM7 region of GlyT2 with other members of the Na⁺/Cl⁻-dependent neurotransmitter transporters reveals that residue W482 is only found at the equivalent position in GlyT1 and GlyT2, while Y491 and N509 are highly conserved throughout this superfamily. Residue S510 is conserved in taurine, GABA and dopamine transporters.

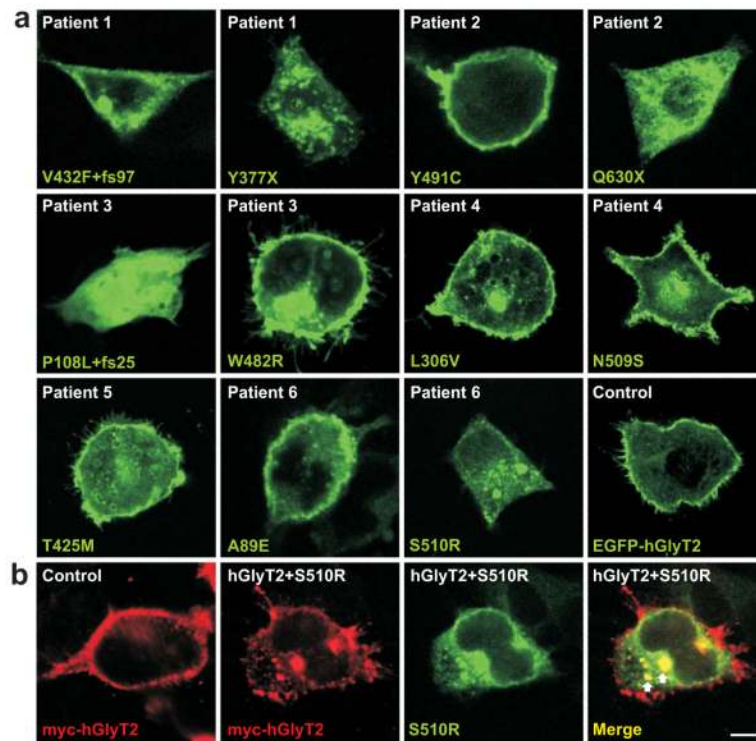


Fig. 2. Subcellular localisation of EGFP-hGlyT2 and hyperekplexia mutants
a, Confocal microscopy of transfected HEK293 cells showing subcellular localisation of EGFP-hGlyT2 and single hyperekplexia mutants and the A89E variant. Confocal microscopy was performed using a Zeiss Axioscop LSM 510 Meta confocal microscope with 40× objective and 3× digital zoom. Note all mutants show distinct expression at the cell surface except P108L+fs25, Y377X, V432F+fs97, Q630X and S510R, which are cytoplasmic. **b**, co-expression experiments reveal that while myc-tagged hGlyT2 is expressed at the cell surface (left panel) mutant S510R traps myc-tagged hGlyT2 in intracellular aggregates (arrows in merged image). Scale bar = 10 μm.

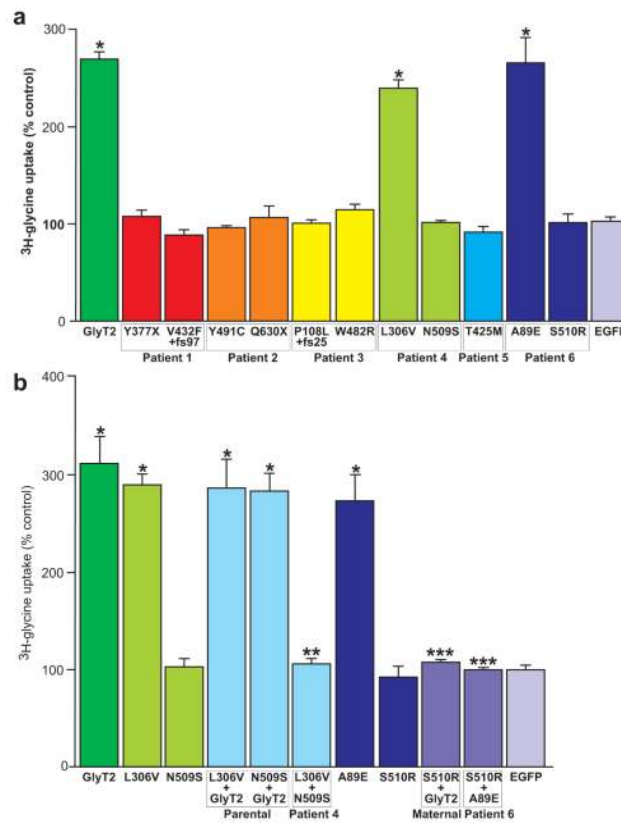


Fig. 3. Transport activity of hGlyT2 and hyperekplexia mutants

a, glycine uptake in HEK293 cells transiently expressing EGFP-hGlyT2 and single hyperekplexia mutants after 5 min incubation with [³H]glycine (60 Ci/mmol, NEN) at a final concentration of 200 μM. **b**, selected pairwise mutant combinations and controls. Since low levels of glycine uptake are found in HEK293 cells³⁰, [³H]glycine uptake was calculated as nmoles/min/mg protein then expressed as a percentage of the pEGFP-C1 (empty expression vector; EGFP) transfected control. Data are means ± s.e.m. (n = 6-20). Statistical comparisons were made using an unpaired Students t-test. * indicates significantly different from EGFP, ** significantly different from L306V, *** significantly different from GlyT2 or A89E. P<0.01.

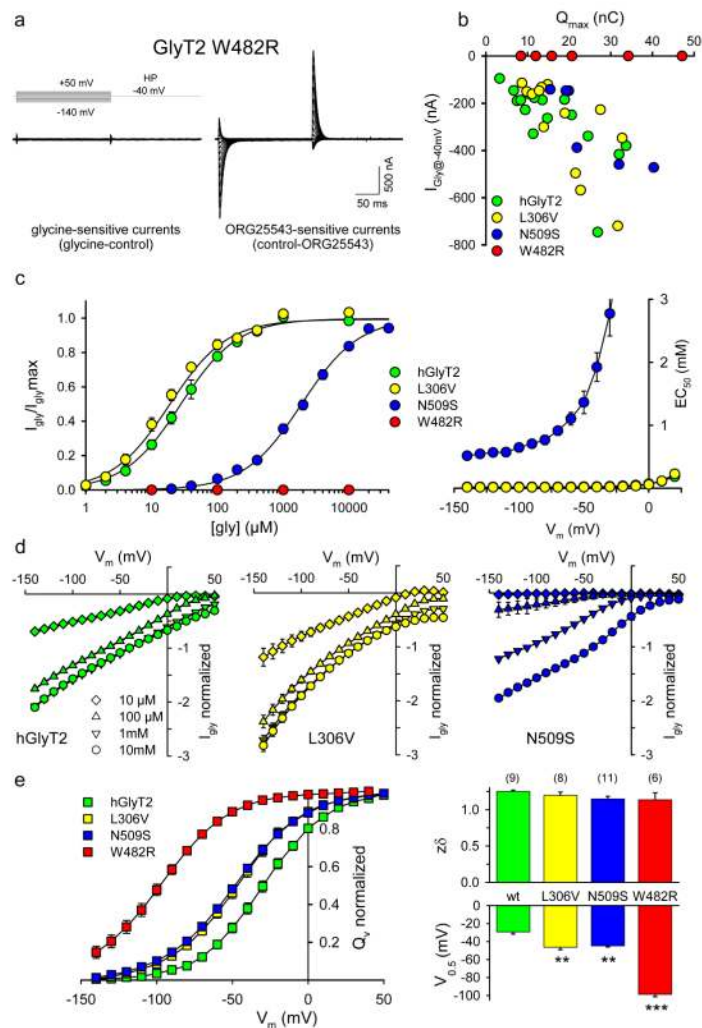


Fig. 4. Electrophysiological characterization of hGlyT2 mutants

a, Steady-state (I_{gly}) and transient currents of W482R are insensitive to glycine (10 mM, left) while ORG25543 (5 μM) blocked Na^+ -dependent transient currents (right). HP: holding potential. **b**, Plot of I_{gly} (-40 mV) and ORG25543-sensitive charge movement relationship for hGlyT2 and mutants. I_{gly} are evoked with applications of [Gly] = 1 mM (hGlyT2, L306V) or [Gly] = 10 mM glycine (N509S, W482R). Q_{max} are obtained as described below. **c**, Left: glycine dose-response curves of I_{gly} for hGlyT2 and mutants. EC_{50} values were $26.9 \pm 3.3 \mu M$ (hGlyT2), $18.8 \pm 1.5 \mu M$ (L306V) and $1923.8 \pm 227.7 \mu M$ (N509S) at -40mV; $22.5 \pm 3.15 \mu M$ (hGlyT2), $15.9 \pm 1.2 \mu M$ (L306V) and $913.1 \pm 72.16 \mu M$ (N509S) at -70mV. Curves are fitted with the equation $I_{gly} = I_{gly,max}/(1 + EC_{50}/[gly])$ and normalized to $I_{gly,max}$ ($n = 3-5$). Right: Plot of glycine EC_{50} - V_m relationship for hGlyT2 and mutants. **d**, Normalized I_{gly} - V_m curves for hGlyT2 and mutants. I_{gly} were normalized to the glycine (10 mM)-evoked currents recorded at -40 mV ($n = 3-7$). **e**, left: Normalized Q_{Vm} - V_m relationships for hGlyT2 and mutants. Q_{Vm} are the time-integrals of ORG25543-sensitive transient currents. Q_{Vm} - V_m curves are fitted to the Boltzmann equation: $Q_{Vm} = Q_{min} + Q_{max}/[1 + \exp(0.03 z\delta (V_{0.5} - V_m))]$ and normalized to Q_{max} . Right: Histograms of the mean $z\delta$ (top) and $V_{0.5}$ (bottom) for hGlyT2 and mutants. $z\delta$ values were 1.25 ± 0.02 (hGlyT2), 1.20 ± 0.05 (L306V), 1.15 ± 0.04 (N509S) and 1.14 ± 0.1 (W482R); $V_{0.5}$ values were -29.3 ± 2.44 (hGlyT2), -46.4 ± 2.7 (L306V), -44.8 ± 1.25 (N509S) and -9.8 ± 2.75 (W482R).

(W482R). Statistical comparisons were made using a paired F-Test, ** indicates $p < 0.01$; *** $p < 0.001$, means \pm s.e.m., with n = number of oocytes).

Table 1
Mutations in the human GlyT2 gene (SLC6A5) in patients with hyperekplexia

Patient	Global origin	Parental origin	Sequence change	Exon	Mutation	Subcellular location	Glycine transport	Mechanism
1	Canada	Paternal Maternal	C1131A G1294T + Ins(T)1295	7 8	Y377X V432F+fs97	Cytoplasmic Cytoplasmic	Abolished Abolished	In frame stop codon, <i>protein truncation</i> Missense plus frameshift, <i>protein truncation</i>
2	USA	Unknown	A1472G C1888T	9 13	Y491C Q630X	Cell surface Cytoplasmic	Abolished Abolished	Missense, <i>functionally inert</i> In frame stop codon, <i>protein truncation</i>
3	Australia	Unknown	delC(319-324) T1444C	2 9	P108L+fs25 W482R	Cytoplasmic Cell surface	Abolished Abolished	Missense plus frameshift, <i>protein truncation</i> Missense, <i>glycine binding site (W482R)</i>
4	Netherlands	Paternal Maternal	C916G A1526G	5 10	L306V N509S	Cell surface Cell surface	Abolished in <i>L306V+fs209S</i>	Missense, <i>sodium binding site (N509S)</i> , <i>compound recessive</i>
5	Netherlands	Paternal Maternal	C1274T C1274T	8 8	T425M T425M	Cell surface	Abolished	Missense, <i>functionally inert</i>
6	UK	Maternal	T1530G	10	S510R	Cytoplasmic	Abolished	Missense mutation, <i>S510R forms large intracellular aggregates, dominant-negative</i>